Research Square

Preprints are preliminary reports that have not undergone peer review.
They should not be considered conclusive, used to inform clinical practice,
or referenced by the media as validated information.

Thermal Performance of Glazing vs Insulated Curtain-Wall Panels in Hot-Arid Urban Environments: Implications for Climate-Adaptive Façade Design

Muhammad Tayyab Naqash
Islamic University of Madinah
Antonio Formisano
antoform@unina.it
University of Naples Federico II

Research Article

Keywords: thermal performance, uPVC frame, curtain walls, insulated infill panel, double-glazed unit (DGU), ISO 10077-2, COMSOL Multiphysics, linear thermal transmittance

Posted Date: November 12th, 2026

DOI: https://doi.org/10.21203/rs.3.rs-11473323/v1

License: This work is licensed under a Creative Commons Attribution 4.0 International License.
Read Full License

Additional Declarations: No competing interests reported.

Thermal Performance of Glazing vs Insulated Curtain-Wall Panels in Hot-Arid Urban Environments: Implications for Climate-Adaptive Façade Design

Muhammad Tayyab Naqash[1], Antonio Formisano[2]*,

[1] Department of Civil Engineering, Islamic University of Madinah, Saudi Arabia, ORCID: 0000-0002-6323-7027, Email: mnaqash@iu.edu.sa, engr.tayyabnaqash@gmail.com

[2] Department of Structures for Engineering and Architecture, School of Polytechnic and Basic Sciences, University of Naples Federico II, Naples, Italy, ORCID: 0000-0003-3592-4011, Email: antoform@unina.it, * Correspondence: engr.tayyabnaqash@gmail.com;

Abstract: The thermal performance of glazed façade systems is a key driver of building energy demand and indoor thermal comfort, particularly in hot climates. This study numerically evaluates steady-state heat transfer in a representative uPVC-framed window/curtain-wall-like glazed façade section detail by comparing two infill configurations: (i) an opaque insulated infill panel and (ii) a gas-filled double-glazed unit (DGU) including the edge/spacer region. A two-dimensional finite-element model was developed in COMSOL Multiphysics and formulated in accordance with ISO 10077-2:2012 to extract the section thermal conductance, L_{2D}, the frame thermal transmittance, Uf (insulated-panel case), and the linear thermal transmittance, ψ (DGU case). Under Madinah summer boundary conditions (Ti = 24 °C, Te = 45 °C), the insulated-panel configuration yielded $L_{2D} = 0.240$ W/(m·K) and $U_f = 0.405$ W/(m²·K), with a negligible linear thermal transmittance $\psi \approx 0.00$ W/(m·K). In contrast, the DGU configuration increased the section conductance to $L_{2D} = 0.352$W/(m·K) and produced $\psi = 0.061$W/(m·K), indicating a measurable edge thermal bridge at the frame–

glazing junction. These findings provide quantitative guidance for façade selection strategies in hot-arid urban environments, contributing to energy-efficient land development and climate-adaptive building design in rapidly urbanizing regions. In cooling-dominated cities characterized by extensive glazed high-rise developments, heat transfer or heat gains can accumulate at the district scale, influencing urban energy demand and resilience to extreme heat.

Keywords: thermal performance; uPVC frame; curtain walls; insulated infill panel; double-glazed unit (DGU); ISO 10077-2; COMSOL Multiphysics; linear thermal transmittance.

1. Introduction

Glazed façade and curtain-wall systems influence building cooling demand and indoor comfort, particularly in hot climates. Beyond center-of-glazing or center-of-panel performance, heat transfer is often governed by the frame region and by thermal bridges at junctions such as the frame–glazing edge, where highly conductive components (e.g., spacers or reinforcements) can increase heat flow and reduce interior surface temperatures [1], [2], [3]. Many published assessments report area-averaged indicators (e.g., U_g, U_p) and therefore may underrepresent perimeter effects that accumulate with glazing length. ISO 10077 [2] provides a section-based framework to quantify these 2D and linear effects through the two-dimensional conductance L_{2D}, the frame transmittance U_f, and the linear thermal transmittance ψ [4], [5]. Section-based thermal bridge modeling, as specified in ISO 10077, has been widely adopted to improve the accuracy of window-frame and façade thermal assessments beyond simplified area-weighted indicators. Malvoni et al. (2016) demonstrated that two-dimensional numerical modelling provides more reliable predictions of frame-region heat transfer than conventional simplified approaches, particularly in the presence of complex cavity geometries. Similarly, Mohammed et al. (2024) emphasised the importance of detailed thermo-environmental modelling of envelope components to accurately capture localised heat-transfer effects that influence overall building performance [6], [7], [8]. Recent large-scale experimental investigations have

demonstrated the effectiveness of passive and hybrid cooling systems in mitigating extreme heat in urban environments. Montero-Gutiérrez et al. (2026) [9] reported that integrated passive cooling and thermal storage systems reduced outdoor air temperatures by more than 15 °C during extreme heat events while maintaining acceptable thermal comfort conditions. Climate-responsive envelope design remains critical in extreme environments. Das et al. (2025) [10] demonstrat, through year-long field measurements in the lower Himalayan cold region, that vernacular buildings exhibited lower heat loss (1.1 W/m²), greater thermal inertia, and fewer discomfort hours than medieval constructions, highlighting the performance consequences of material and assembly transitions.

Authors in [10] reviewed emerging glazing configurations to improve energy efficiency and daylight performance, noting that spacer materials and edge detailing significantly influence overall thermal performance. Calautit et al. further demonstrated, through experimental and techno-economic analyses, that secondary and advanced glazing systems can substantially alter envelope heat transfer characteristics, underscoring the importance of accurately modelling edge-region components in façade simulations. The objectives are to: (a) compute L_{2D} for both configurations; (b) derive U_f for the insulated-panel case; and (c) quantify ψ for the DGU case to isolate the glazing-edge thermal bridge and identify detailing priorities for improved façade performance.

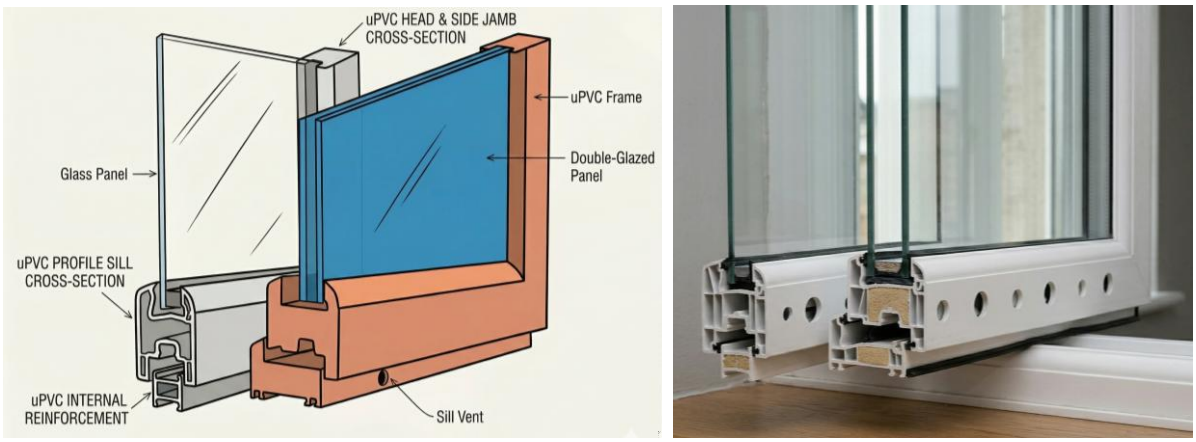


Figure 1. uPVC-framed insulated panel and double-glazed unit

Figure 1 illustrates the cross-sectional configuration of the investigated uPVC-framed façade element, highlighting the double-glazed unit (DGU), internal steel reinforcement within the uPVC profile, and sill ventilation detailing. The figure emphasises the layered assembly of the glazing system and the structural role of the reinforced frame in resisting bending and in-plane deformation.

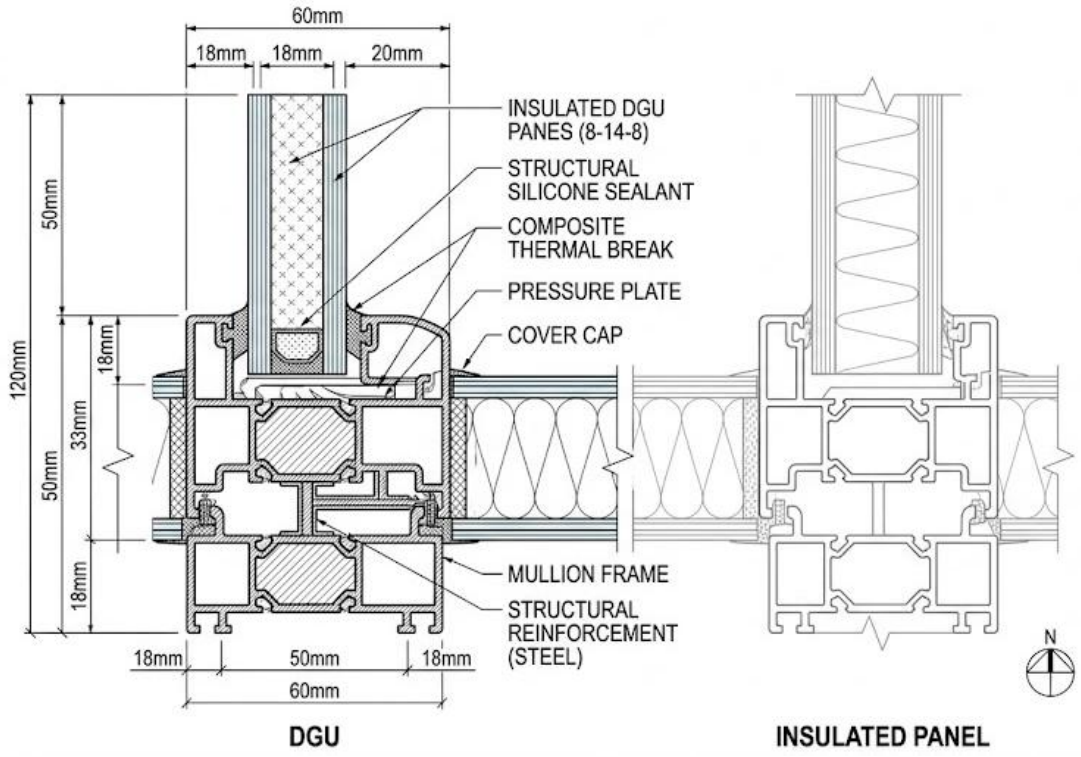


Figure 2: Geometry of the uPVC-framed window/façade section used in the numerical study

Figure 2 shows the geometric configuration of the uPVC façade section adopted in the numerical study, including dimensional parameters and the two investigated infill configurations: (i) an insulated opaque panel and (ii) a conventional gas-filled double-glazed unit (DGU). The figure defines the frame depth, glazing pocket dimensions, and reinforcement location used for structural compatibility assessment. Rapid urbanisation in hot-arid regions has significantly increased cooling-dominated building energy demand, particularly in Middle Eastern and North African cities, where extensive glazed high-rise developments have become prevalent. In such climates, outdoor temperatures frequently exceed comfort thresholds for

extended periods, intensifying reliance on mechanical cooling systems and increasing peak electricity loads.

Integrated urban resilience frameworks further underscore the need to couple building-scale thermal performance with city-scale climate adaptation strategies. Kim et al. (2026) [11] proposed a multiscale assessment system that combines GIS, microclimate simulations, and life-cycle analysis to evaluate urban heat vulnerability and energy efficiency simultaneously. Their approach demonstrates that building envelope performance is not an isolated technical issue but a critical determinant of district-level climate resilience, particularly in cities facing rising cooling demand. In high-density developments, cumulative envelope heat transfer effects can amplify urban energy burdens, necessitating detailed investigations of façade thermal behavior under extreme climatic conditions.

Building envelopes, especially curtain-wall façades with high glazing ratios, play a critical role in determining urban-scale energy performance and resilience to extreme heat events. While centre-of-glazing performance is often emphasized in regulatory frameworks, perimeter heat transfer and linear thermal bridges at frame–glazing junctions can cumulatively contribute to substantial cooling loads when multiplied across large façade areas and dense urban districts. Therefore, understanding and optimizing section-level thermal behavior is not only a component-scale concern but also a strategic consideration for sustainable urban development in hot-arid environments. Passive design strategies for curtain-wall systems have increasingly focused on optimizing façade configuration to reduce cooling demand in warm and subtropical climates. Li et al. (2023) demonstrated that façade orientation, glazing specification, and integrated shading strategies significantly influence thermal comfort and cooling energy demand in curtain-wall office buildings located in subtropical climates (data.cribelab.org). Their findings emphasize that façade performance assessment must move beyond center-of-glass properties and instead consider the complete façade assembly, including frame effects and edge conditions, particularly in cooling-dominated regions . They have highlighted the importance of microclimate-responsive urban design in mitigating thermal stress at the

neighborhood scale. Xu et al. demonstrated that vegetation structure and spatial configuration significantly influence outdoor thermal comfort, resulting in measurable reductions in surface temperatures and improvements in human heat stress indices. Their findings emphasize that building envelope exposure, shading conditions, and surface heat exchange are critical factors in determining localized microclimatic performance. In hot, arid urban contexts, façade characteristics and heat transfer properties directly affect both indoor cooling demand and outdoor heat accumulation, underscoring the need to evaluate envelope-level thermal behavior within broader urban climate adaptation strategies [12].

Urban block morphology has been shown to significantly influence building energy performance by controlling solar exposure and envelope interactions. Fang et al. (2025) quantitatively demonstrated that parameters such as floor area ratio, mean building height, and orientation strongly affect solar availability across façades in high-density residential districts. While their research focused on severe cold climates and solar gains, the underlying principle that block geometry modulates façade-level energy exchange remains equally relevant for hot-arid regions. In climates dominated by cooling demand, the same morphological characteristics that enhance solar gain in cold regions may intensify heat accumulation and increase transmission losses, highlighting the importance of evaluating façade heat transfer performance in dense urban fabrics [13].

Although ISO 10077-based simulations are well established for window-frame analysis, limited studies explicitly quantify the differential impact of glazing-edge aluminium spacers versus insulated opaque infill panels under identical boundary conditions in hot-climate contexts. The novelty of this work lies in (i) isolating the linear thermal transmittance contribution of the aluminium spacer region using a controlled geometric comparison, (ii) establishing a $\psi \approx 0$ baseline using an insulated opaque panel within the same frame, and (iii) quantifying the relative increase in L2D and minimum interior surface temperature reduction attributable solely to glazing-edge detailing under extreme summer conditions (Madinah climate). This controlled comparison enables clearer identification of edge-driven thermal

penalties in façade systems [3], [14], [15], [16], [17]. This investigation complements previous structural and façade system studies on aluminium curtain-wall configurations (Formisano & Naqash, 2024; Naqash & Formisano, 2024), extending the discussion from structural performance to detailed section-level quantification of thermal bridges.

This study applies a two-dimensional, ISO 10077-2-consistent finite-element workflow in COMSOL Multiphysics [18] to evaluate a representative uPVC frame section under Madinah summer boundary conditions. Two infill configurations are compared using identical geometry and boundary conditions: (i) an insulated opaque infill panel and (ii) a gas-filled double-glazed unit (DGU) with explicit representation of spacer/seal edge components. Recent advances in glazing technologies highlight the growing complexity of window systems and the need for more detailed performance-prediction methods.

2. Modeling and assumptions

2.1 Cavity heat-transfer formulation

The COMSOL model solves 2D steady-state heat conduction through the frame and glazing/panel domains, with prescribed summer boundary temperatures representative of Madinah: interior air temperature $\boldsymbol{T_i}$ = 24 °C and exterior air temperature $\boldsymbol{T_e}$ = 45 °C. Surface heat exchange is represented using standard surface (film) resistances/coefficients.

For single-pane glazing, heat transfer occurs through (i) surface heat exchange at the interior and exterior surfaces and (ii) conduction through the glass. No inter-pane cavity exists; therefore, the cavity correlations below are not required for the glazing itself (they may still be used for any frame cavities present). For a double-glazed unit (DGU), heat transfer across the inter-pane gas space is not resolved using CFD. Instead, the gap is modeled using an ISO-consistent equivalent cavity heat-transfer coefficient that combines conduction/natural convection and long-wave radiation. The total effective gap coefficient is shown by EQ (1).

$$h_{\text{gap}} = h_a + h_r \qquad EQ\ (1).$$

and the corresponding gap heat flux (per unit area) is shown by EQ (2).

$$q_{\text{gap}} = h_{\text{gap}}(T_1 - T_2) \qquad EQ\ (2)$$

Where $\boldsymbol{T_1}$ and $\boldsymbol{T_2}$ are the temperatures of the two facing glass surfaces, $\boldsymbol{h_a}$ accounts for conduction and natural convection in the gap, and $\boldsymbol{h_r}$ accounts for radiative exchange between the facing surfaces. These $\boldsymbol{h_a}$ and $\boldsymbol{h_r}$ expressions are applied to the inter-pane cavity in the DGU (and analogously to frame cavities where the equivalent-cavity approach is adopted), enabling efficient steady-state simulations consistent with ISO 10077 practice without full buoyant-flow CFD.

2.2 Cases considered

Two configurations are analyzed using the same uPVC frame cross-section and identical boundary conditions, so that differences in heat transfer can be attributed primarily to the infill type and its edge detailing. Figure 3 presents the ISO 10077-- 2–consistent numerical workflow used to evaluate the thermal behaviour of the insulated panel and DGU configurations within the same uPVC frame geometry. The procedure comprises geometry definition, assignment of material properties, implementation of equivalent cavity models, application of ISO surface resistances, steady-state finite-element solution in COMSOL Multiphysics, and post-processing to extract section conductance L_{2D}, frame transmittance U_f, and linear thermal transmittance ψ. The standardized workflow ensures that differences in results are attributable solely to the infill configuration and edge detailing.

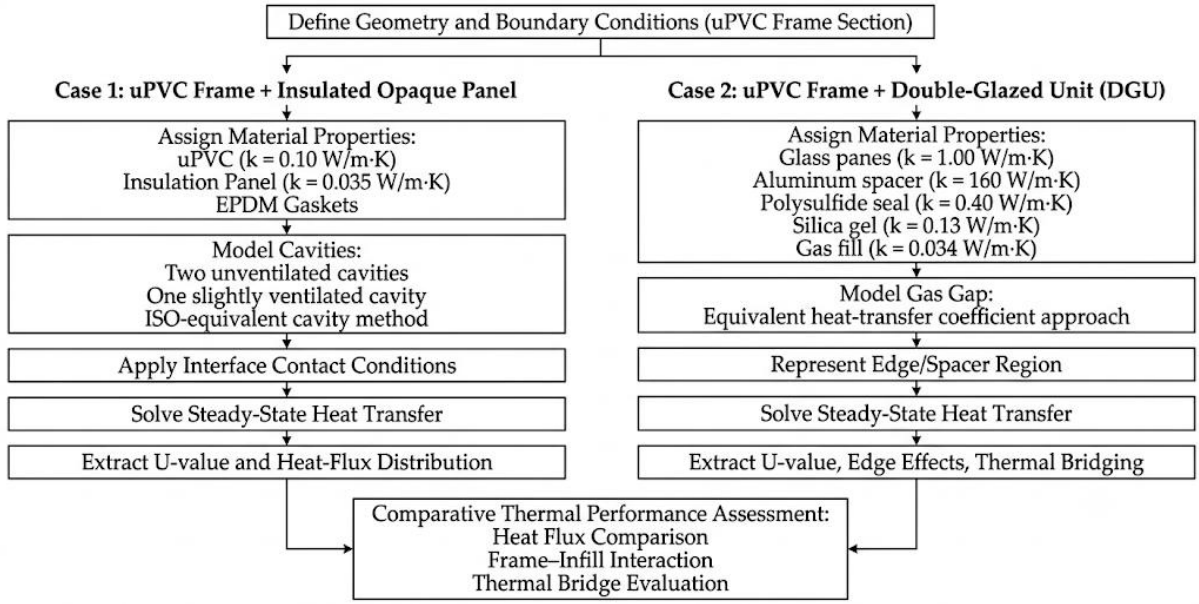


Figure 3. ISO 10077-2–consistent thermal modeling workflow adopted for the two investigated uPVC frame configurations: (i) insulated opaque infill panel and (ii) gas-filled double-glazed unit (DGU).

Case 1: uPVC frame with insulated infill panel (opaque panel replacing glazing).

In this case, the glazing region is replaced by an opaque insulation panel. The frame is modeled as uPVC (thermal conductivity $\boldsymbol{k}$ = 0.10 [W/(m K)]), with EPDM gaskets to ensure contact and sealing. EPDM blocks are positioned on both sides of the insulation panel, as in the reference section detail. The insulation panel has a thermal conductivity $\boldsymbol{k}$ = 0.035 W/(m K). The section includes three cavities: two are fully closed and treated as unventilated, and one is slightly ventilated. Cavities are modelled using the adopted ISO-consistent equivalent-cavity approach.

Case 2: uPVC frame with conventional double-glazed unit (DGU).

In this case, the insulated panel is replaced by a conventional gas-filled DGU installed within the same uPVC frame geometry, including representation of the edge/spacer and seal region. The DGU consists of two glass panes with thermal conductivity $\boldsymbol{k}$ = 1.00 [W/(m K)]. Edge-region components include an aluminium spacer and associated sealing/desiccant materials (modelled as aluminium, polysulfide, and silica gel) with thermal conductivities of 160, 0.40,

and 0.13 [W/(m · K)], respectively. The inter-pane space is filled with a gas with a thermal conductivity of 0.034 [W/(m K)]. The gas gap is modeled using the equivalent heat-transfer coefficient described in Section 2.1 rather than as a resolved flow field.

2.3 Boundary conditions

Heat exchange at interior and exterior surfaces is modeled using Newton's law of cooling (convective boundary condition) as shown in EQ(3):

$$-\mathbf{n} \cdot (-k\nabla T) = h\,(T_\infty - T) \qquad \text{EQ(3).}$$

Where $\boldsymbol{k}$ is thermal conductivity, T is the local surface temperature, $\boldsymbol{T}_\infty$ is the adjacent air temperature (interior or exterior), and h is the surface heat-transfer coefficient.

Following ISO practice, $\boldsymbol{h}$ is related to the surface thermal resistance $\boldsymbol{R_s}$ by $\boldsymbol{h = 1/R_s}$. The adopted boundary temperatures (Madinah summer) are: interior air temperature, Ti = 24 °C; exterior air temperature, Te = 45 °*C.* The adopted surface resistances are [note the units are (m²·K)/W]: Normal internal surface resistance: $\boldsymbol{R_{si,n}}$ = 0.13 m^2K/W, Protected internal surface resistance: $\boldsymbol{R_{si,p}}$ = 0.2 (m^2K/W). External surface resistance: R_{se} = 0.04 m^2K/W. Equivalently, the corresponding film coefficients are: $\boldsymbol{h_{i,n}}$ = 1/0.13 = 7.69 [W/(m^2 K)], $\boldsymbol{h_{i,p}}$ = 1/0.20 = 5.00 [W/(m^2 K)] and $\boldsymbol{h_e}$= 1/0.04 = 25.0 [W/(m^2 K)]. Protected resistances are applied to "corner/protected" interior boundaries, per ISO guidance, to represent reduced convection at edges.

2.4 2D thermal conductance and transmittance

After solving for the steady-state temperature field, the total heat flow rate per unit depth, Φ (W/m), crossing the section is obtained by integrating the normal total heat flux over the interior boundary. The two-dimensional thermal conductance is computed as shown in EQ(4):

$$L_{2D} = \Phi/(T_e - T_i) \qquad \textit{EQ(4).}$$

In COMSOL, $\boldsymbol{\Phi}$ is evaluated using a boundary integration operator applied to the normal component of the total heat flux. For the insulated infill case, the frame transmittance is computed using EQ(5):

$$U_f = \frac{L_{2D} - U_p\, b_p}{b_f} \qquad EQ(5).$$

where U_p is the transmittance of the central panel area, $\boldsymbol{b_p}$ is the visible panel width, and $\boldsymbol{b_f}$ is the projected frame width for the 2D section. The insulated-panel transmittance U_p includes the panel thermal resistance and the interior/exterior surface resistances. With panel thickness $\boldsymbol{d_p}$ and conductivity $\lambda_p R_p = \frac{d_p}{\lambda_p}$

Normal and protected panel transmittances are shown by EQ(6) and EQ(7), respectively. :

$$U_{p,n} = \frac{1}{R_p + R_{si,n} + R_{se}} \qquad EQ(6)$$

$$U_{p,p} = \frac{1}{R_p + R_{si,p} + R_{se}} \qquad EQ(7)$$

A weighted U_p is used to account for protected-edge portions (e.g., 30 mm) consistent with the benchmark setup. For the glazing configuration, ISO-style post-processing separates the 2D heat flow into contributions from the frame and from the central glazing area. The remaining excess heat flow is attributed to the edge effect and reported as the linear thermal transmittance, as shown in EQ (8).

$$\psi = L_{2D} - U_f\, b_f - U_g\, b_g \qquad EQ(8).$$

Where $\boldsymbol{U_g}$ is the center-of-pane glazing transmittance, and $\boldsymbol{b_g}$ is the visible glazing width for the section.

3. Numerical model and methodology

A two-dimensional steady-state heat-transfer model was developed to investigate the thermal performance of a representative curtain-wall/window-type frame section. Two test cases were considered to isolate the influence of the infill type while keeping the same frame geometry:

- Insulated infill panel case: the glazing region is replaced by an opaque insulation panel.
- Double-glazed unit (DGU) case: a conventional DGU is installed, including edge components (spacer/seal region).

By comparing these two cases under identical boundary conditions, the influence of the infill type and edge region on the overall section heat transfer can be quantified. After solving for the steady-state temperature field, the model is post-processed to compute thermal-bridge metrics consistent with ISO 10077 procedures. In particular, the two-dimensional thermal conductance $\boldsymbol{L_{2D}}$ is obtained from the integrated heat flow rate through the section, and derived quantities such as the frame thermal transmittance U_f (insulated-panel case) and the linear thermal transmittance $\boldsymbol{\psi}$ (glazing case) are evaluated from the corresponding ISO-style relations.

3.1 Assumptions

The following assumptions are adopted to simplify the analysis while maintaining consistency with standard steady-state thermal-bridge evaluation practice:

- Steady-state conditions: temperatures and heat fluxes do not vary with time.
- Homogeneous/isotropic materials: each solid domain is assigned a constant thermal conductivity for the steady-state solution.
- Two-dimensional approximation: the section is modeled per unit out-of-plane depth (1 m), neglecting 3D effects such as fasteners and local discontinuities not represented in the cross-section.

- Equivalent cavity modeling: frame cavities and the DGU gas gap are not solved using CFD; instead, they are modeled using ISO-consistent equivalent heat-transfer coefficients or equivalent conductivities that account for conduction, natural convection, and long-wave radiation.
- Prescribed interior/exterior air temperatures with film resistances: interior and exterior environments are represented by air temperatures and surface resistances (film coefficients), applied as convective boundary conditions.

Protected internal resistances are applied on interior "protected" boundaries near corners/returns following ISO guidance. Two boundaries are treated as adiabatic (symmetry/no-flux) in accordance with the benchmark setup: the wall boundary and the end boundary of the panel/glazing region.

3.2 Boundary heat flux condition

The boundary temperatures representative of Madinah summer conditions are:

- Interior air temperature: $\boldsymbol{T_i} = 24\,\mathbf{°C}$
- Exterior air temperature: $\boldsymbol{T_e} = 45\,\mathbf{°C}$

In accordance with ISO practice, the heat-transfer coefficient is defined in terms of the surface resistance. $\boldsymbol{R_s}$ by: $\boldsymbol{h = 1/R_s}$. Simulations were performed in COMSOL Multiphysics using the Heat Transfer Module with the Heat Transfer in Solids and Fluids interface. A 2D steady-state formulation was used, corresponding to a unit out-of-plane depth of 1 m. The temperature field was discretized using quadratic Lagrange elements to improve accuracy in regions with strong gradients and thin components (e.g., spacer/seal regions). Two configurations were analyzed in COMSOL Multiphysics.

Configuration A: insulated infill panel.: A representative frame cross-section composed primarily of uPVC with EPDM gaskets and internal cavities; an insulation panel replaces the glazing region. Key dimensions include:

- Visible panel width: b_p = 190 mm.
- Panel thickness: d_p = 28 mm.
- Projected frame width: b_f = 110 mm.
- Frame height: d_f = 83 mm.

Configuration B: double-glazed unit (DGU). The DGU and edge-region components replace the insulated panel. Key parameters include:

- Visible glazing width: b_g = 190 mm.
- Total glazing thickness: d_g = 28 mm
- Glass thickness: d_t = 4 mm (two panes)
- Filling gas conductivity: k = 0.034 W/ (m K)
- Aluminum spacer thickness: a_t = 0.5 mm.
- Polysulfide block width: p_w = 3 mm.
- Silica gel block: 9 x 19 mm.

3.3 Materials and Modeling

The material properties adopted in the model are summarised in Table 1. All materials are assumed homogeneous and isotropic, and thermal conductivity is assumed constant for the steady-state simulations.

Table 1. Material properties adopted in the model.

Material	Thermal conductivity k[W/(m·K)]
uPVC	0.10
EPDM	0.25
Insulation panel	0.035
Glass	1.00
Aluminum	160
Polysulfide	0.40

Polyamide	0.25
Silica gel	0.13

Frame cavities were not solved as buoyant-flow CFD domains. Instead, they were represented by ISO-consistent equivalent cavity models that account for conduction, natural convection, and radiation. Unventilated cavities were modeled using an equivalent thermal conductivity k_{eq} (or an equivalent heat-transfer coefficient formulation), computed from analytical expressions for convective/conductive and radiative components. Slightly ventilated cavities were modeled by increasing the effective conductivity relative to the corresponding unventilated cavity, consistent with the benchmark rule (doubling k_{eq}). In the radiation model, the surface emissivity is set to $\varepsilon = 0.9$. Unstructured triangular meshes were used. The insulated-panel configuration employed a mesh with 854 triangles (minimum element quality approximately 0.59).

In comparison, the glazing configuration used a finer mesh with 2687 triangles (minimum element quality approximately 0.56) to resolve thin spacer and seal regions. A mesh-refinement sensitivity check was performed, confirming that additional refinement reduced L_2D by less than 1%, indicating mesh-independent results.A stationary nonlinear solver with direct linearization was used, with a relative tolerance of 10^{-6}.

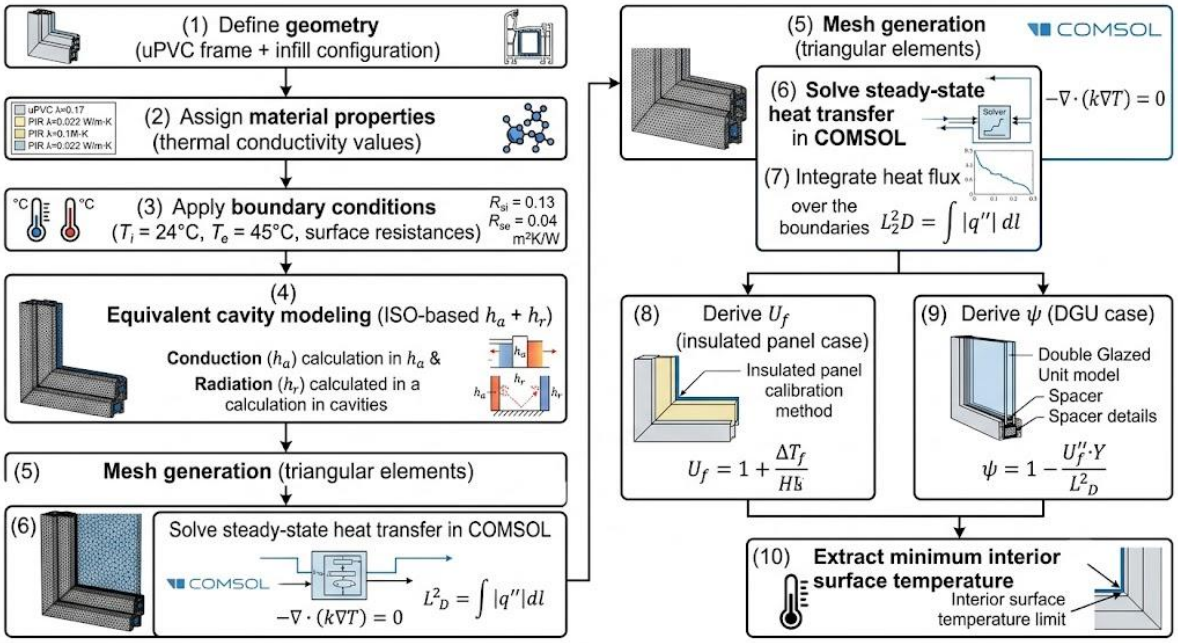


Figure 4. Workflow of ISO 10077-2, consistent numerical modeling, and post-processing procedure adopted in this study.

Figure 4 summarizes the ISO 10077-2-based numerical workflow adopted in this study. The procedure includes defining geometry, assigning materials, applying boundary conditions, modeling equivalent cavities, generating a mesh, and solving for steady-state in COMSOL. Post-processing steps involve the integration of the heat flux to determine L_{2D}, followed by the derivation of U_f and ψ, and extraction of minimum interior surface temperatures.

4. Results and Discussion

This section presents the computed thermal-bridge metrics for the two investigated configurations (insulated infill panel and DGU) using the same uPVC frame cross-section and identical Madinah summer boundary conditions. Table 2 summarizes the computed section thermal conductance and the derived frame thermal transmittance for the insulated infill-panel configuration.

Table 2. Thermal properties for the frame with an insulated infill panel.

Quantity	Value	Unit

L_{2D}	0.24	W/(m·K)
U_f	0.405	W/(m²·K)
ψ	0.00	W/(m·K)

As expected, the insulated infill panel configuration produces a negligible linear thermal transmittance ($\psi \approx 0$ W/(m • K)), since no glazing-edge thermal bridge is present. Heat transfer is governed primarily by the frame and cavity regions. The relatively low L2D confirms that the opaque insulated panel reduces perimeter heat flow compared with the glazing configuration. The value $\boldsymbol{U_f} = 0.405$ W/(m²·K) indicates that, even with an insulated opaque infill, the frame region and its internal cavities contribute substantially to overall heat transfer. This behaviour is typical of frame-dominated assemblies and suggests that improving the infill insulation alone may not be sufficient; optimising the uPVC frame geometry, cavity treatment, and sealing/gasket detailing remains important to reduce heat transfer and improve interior surface temperatures.

Compared with the insulated-panel case, the section thermal conductance increases from 0.240 to 0.352 W/(m·K), corresponding to an increase of 0.112 W/(m·K), i.e., approximately 47% relative to the insulated-panel baseline, under identical boundary conditions. This increase reflects additional heat-transfer pathways associated with the glazing region and, critically, the highly conductive aluminium spacer in the perimeter edge zone (k = 160 W/(m·K)). The aluminium spacer creates a localized conductive bridge between interior and exterior glass panes, intensifying heat flux at the glazing edge. For the DGU configuration, the derived thermal-bridge metrics are reported in Table 3.

Table 3. Thermal properties for the frame with DGU.

Quantity	Value	Unit
L_{2D}	0.352	W/(m·K)
$\boldsymbol{\psi}$	0.061	W/(m·K)

Figure 5 provides a conceptual comparison of heat-flow paths in the insulated-panel and DGU configurations. While the opaque panel exhibits relatively uniform heat transfer across the section, the DGU case shows concentrated heat flux at the glazing edge due to the highly conductive aluminum spacer. This localized intensification represents the physical origin of the non-zero linear thermal transmittance ψ observed in the numerical results.

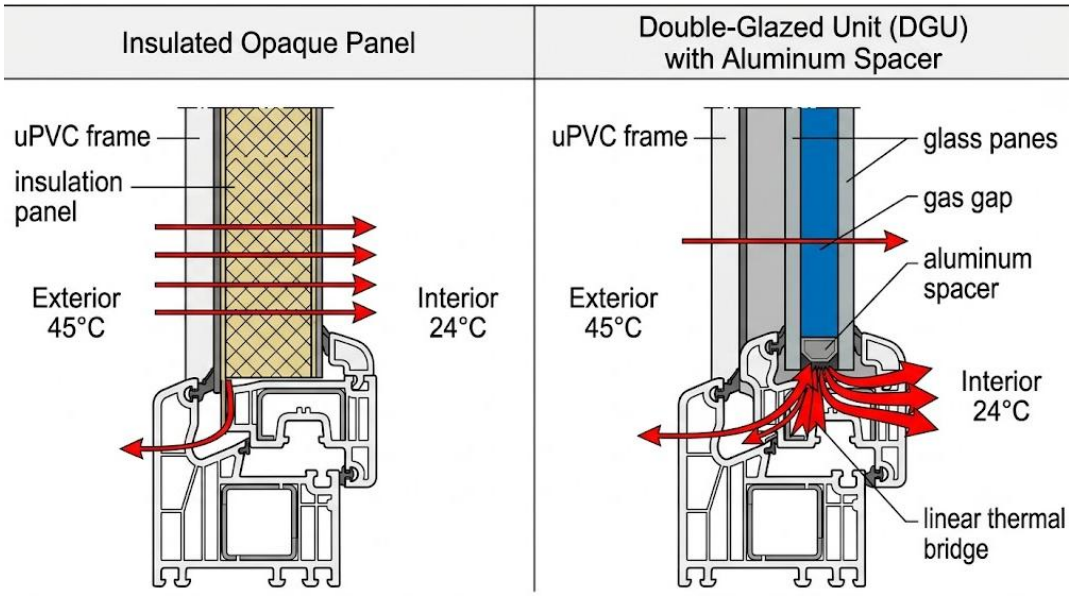


Figure 5. Conceptual comparison of heat-flow paths in an insulated opaque panel (left) and DGU with aluminium spacer (right), highlighting the edge thermal bridge responsible for linear transmittance

The calculated linear thermal transmittance for the frame–DGU interface is $\psi = 0.061$ W/(m·K). This value lies within the commonly reported ranges for conventional aluminum-spacer DGU systems (typically 0.05–0.10 W/(m·K)), but remains higher than those for high-performance warm-edge systems (≈0.02–0.05 W/(m·K)). The non-zero ψ confirms the presence of an edge thermal bridge at the frame–glazing junction. It represents the additional linear heat loss at the frame–glazing junction beyond that accounted for by area-based terms (frame and centre-of-glazing performance). Reducing ψ is important in façade design because edge losses accumulate with perimeter length; warm-edge spacer concepts and improved edge detailing are commonly used to mitigate perimeter heat loss and condensation risk. This confirms a measurable edge thermal bridge attributable to the aluminum spacer and

edge-region materials. In contrast, the insulated-panel configuration yielded $\psi \approx 0$, establishing a reference baseline for glazing-edge comparison. Minimum temperatures were extracted to identify the coldest regions of the section.

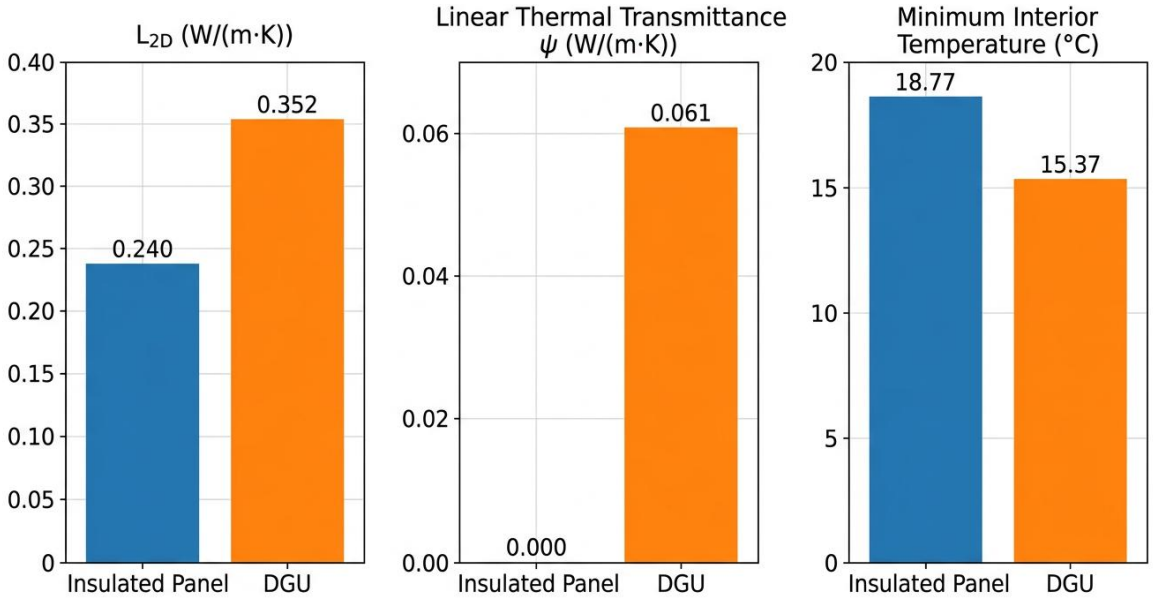


Figure 6: key thermal metrics for both configurations, showing higher L_2D and ψ values and a lower minimum interior temperature for the DGU case.

To provide an integrated comparison of the two façade configurations, Figure 6 summarizes the principal thermal metrics derived from the ISO 10077-2 post-processing procedure. The DGU configuration exhibits a 47% increase in section thermal conductance ($L2D$), a non-zero linear thermal transmittance ($\psi = 0.061$ W/(m·K)), and a 3.40 K reduction in the minimum interior surface temperature relative to the insulated-panel case. The comparative visualization consolidates the findings of current section. Clearly, it demonstrates that glazing-edge detailing significantly alters both global heat-flow indicators and localised surface temperatures under identical boundary conditions.

5. Implications for Sustainable Urban Development in Hot-Arid Regions

Although the benchmark section corresponds to a window-type detail, the findings have broader implications for curtain-wall-dominated urban developments in hot-arid regions. In

rapidly urbanising cities characterised by extensive glazed façades, even modest increases in linear thermal transmittance can accumulate significantly across large façade perimeters and across multiple floors. As cooling demand already represents a major share of total building energy consumption in such climates, perimeter-driven heat gains can exacerbate peak electricity loads, increase operational costs, and intensify urban heat stress. From an urban energy perspective, the 47% increase in section thermal conductance observed when replacing an insulated opaque panel with a conventional DGU illustrates how façade configuration decisions at the component level may scale into meaningful differences in district-level cooling demand. In high-rise developments with continuous glazing bands and repetitive façade modules, edge thermal bridges associated with aluminium spacers and conductive framing systems may contribute to cumulative heat gains that are not fully captured by area-averaged performance indicators alone. The results highlight several design implications:

- Infill choice shifts the dominant heat path. With an opaque insulated panel, heat flow is more concentrated through the frame and adjacent cavity regions; with DGU, additional heat-transfer routes occur through the glazing region and the edge zone.
- Edge effects must be treated explicitly. The non-zero ψ demonstrates that edge thermal bridging can be significant even when centre-of-glazing performance is moderate; for curtain walls with long glazing perimeters, these linear losses can accumulate at building and district scales.
- Material selection influences urban cooling loads. Replacing conventional aluminium spacers with warm-edge (low-conductivity) alternatives and minimising conductive connections in aluminium-based framing systems can reduce perimeter heat gains and improve façade-level resilience to extreme heat.
- Integrated façade optimization is required. Improving Uf typically requires coordinated optimization of cavity treatment, gasket design, and frame material/geometry rather than relying solely on higher-performance glazing units.

- Overall, the study demonstrates that climate-adaptive façade design in hot-arid cities should address both area-based and linear thermal metrics to effectively reduce cooling demand and enhance the thermal resilience of dense urban environments..

Temperature profiles for each configuration are presented in Figures 7 and 8 to illustrate heat-flow paths and the locations of maximum gradients and minimum interior temperatures. These distributions support the interpretation of the global metrics (L_{2D}, U_f, ψ) in terms of local cold spots within the section.

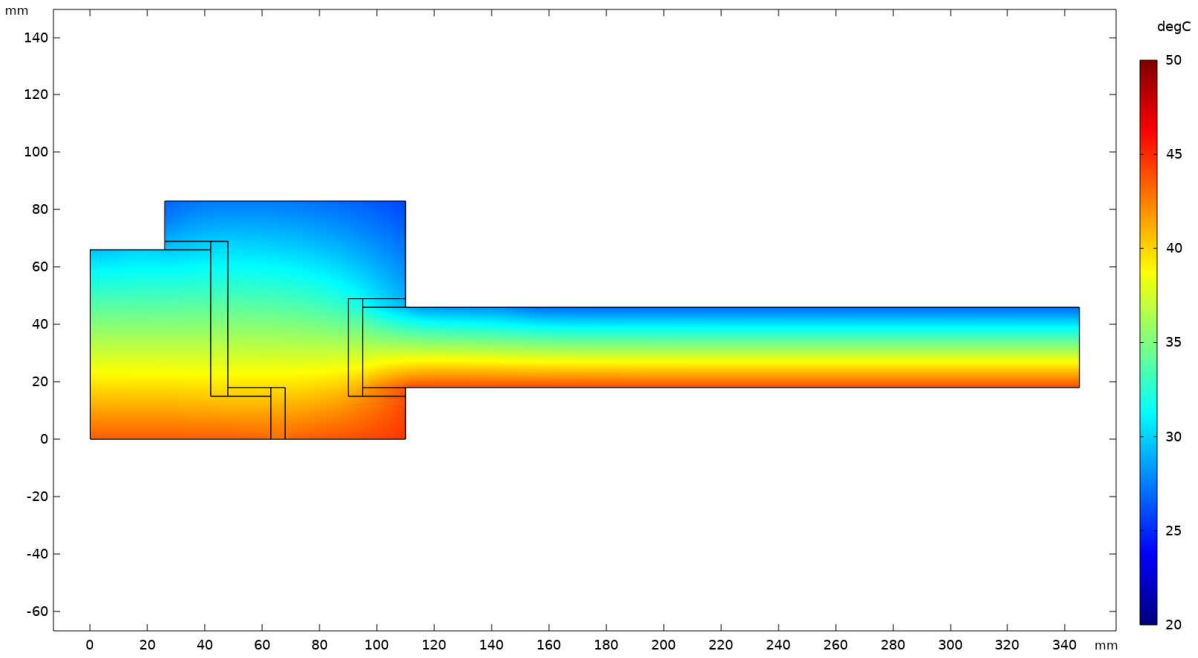


Figure 7. Surface Temperature (°C) for the insulated panel

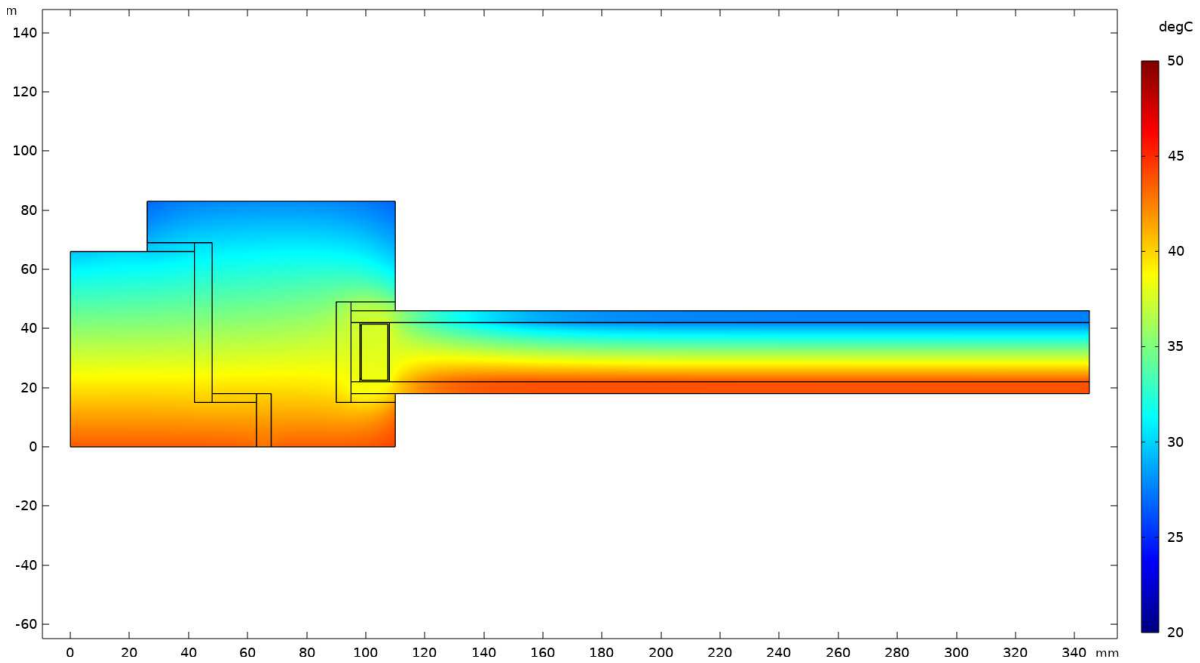
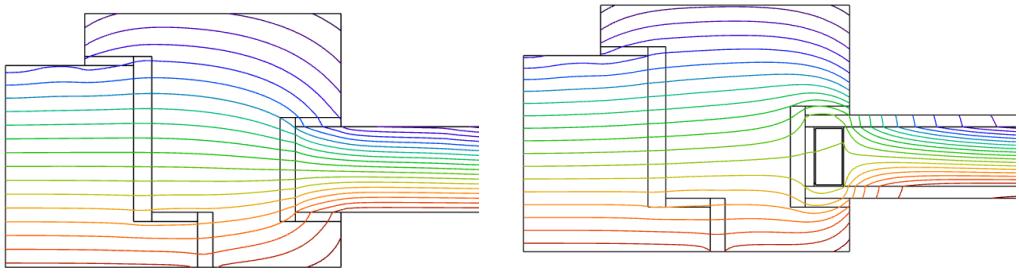


Figure 8. Surface Temperature (°C) for the double-glazed panel

Compared with the insulated infill panel, the DGU case exhibits stronger distortion and crowding of isotherms at the frame–glazing junction, indicating a pronounced edge thermal bridge (higher L_{2D} and non-zero ψ) and lower local interior surface temperatures near the glazing pocket.



Isotherms of an insulated panel (left) Isotherms of a double-glazed panel (right)

Figure 9. Isotherms for isolated panel (left) and double-glazed unit (right)

The insulated infill panel case exhibits relatively smooth, near-parallel isotherms, as shown in Figure 9, indicating a more uniform temperature drop and heat transfer dominated by the uPVC frame and cavities. In contrast, the DGU case shows pronounced bending and crowding of isotherms at the frame–glazing junction, revealing a localized edge thermal bridge associated with the glazing pocket/spacer region. This contour 'pinching' implies higher local heat flux and lower critical interior surface temperatures near the glazing edge, consistent with the increased $\boldsymbol{L_{2D}}$ and the non-zero linear transmittance $\boldsymbol{\psi}$.

6. Conclusions

This study presented a two-dimensional steady-state numerical assessment of a representative uPVC frame cross-section, comparing an insulated infill panel configuration with a gas-filled double-glazed unit (DGU) configuration using COMSOL Multiphysics. The main conclusions are:

- Under the adopted Madinah summer boundary conditions and ISO surface resistances, the insulated infill panel case produced $L_{2D} = 0.240$ W/(m·K), $U_f = 0.405$W/(m²·K), and a negligible linear thermal transmittance $\psi \approx 0$W/(m·K). This confirms that, even with a well-insulated opaque infill, heat transfer remains strongly influenced by the frame and cavity regions.
- Replacing the insulated panel with the DGU increased the section conductance to $L_{2D} = 0.352$ W/(m·K) and yielded a linear thermal transmittance $\psi = 0.061$W/(m·K).
- The approximately 47% increase in L_{2D} demonstrates that glazing-edge components introduce additional heat-transfer pathways beyond area-based performance.
- The temperature contours and isotherms show stronger contours and greater bending at the frame–glazing junction in the DGU case, indicating a localized edge thermal bridge. This is consistent with the non-zero ψ value and with the lower minimum temperature indicator observed for the DGU configuration.

The results also demonstrate that reporting ψ for opaque infill cases (ψ ≈ 0) provides a useful baseline for quantifying the true impact of glazing-edge detailing in façade systems. Overall, the results emphasize that improving façade thermal performance requires not only higher-performing infill elements, but also careful control of edge detailing (e.g., warm-edge spacers and reduced conductive continuity) and frame/cavity design to limit thermal bridging and improve interior surface temperatures. For example, if ψ increases by 0.061 W/(m·K) and a high-rise floor has 400 m of glazing perimeter, the additional linear heat transfer amounts to approximately 24.4 W/K per floor, illustrating the potential cumulative impact at the building scale.

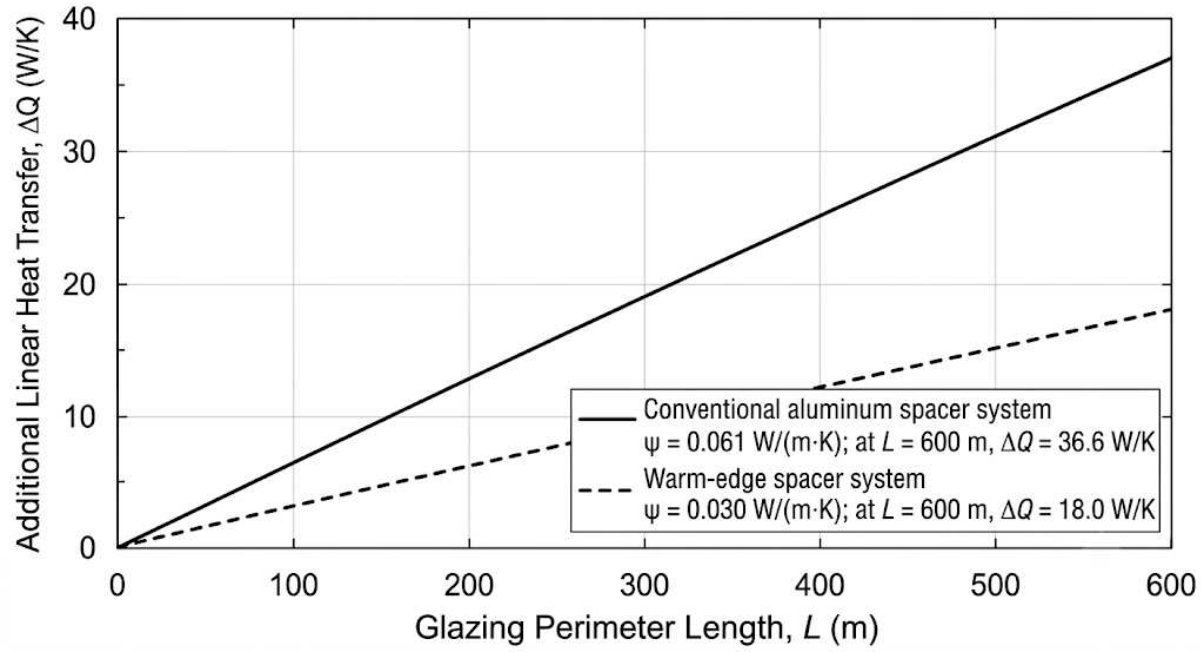


Figure 10. Scaling of additional linear heat transfer as a function of façade glazing perimeter length, comparing conventional aluminum spacer systems (ψ = 0.061 W/(m·K)) and warm-edge spacer systems (ψ = 0.030 W/(m·K)). The linear relationship (ΔQ = ψL) illustrates the cumulative impact of edge thermal bridging in high-rise glazed buildings.

Although the present study evaluates a representative section detail, the scaling analysis highlights how modest increases in ψ can translate into significant cumulative cooling loads at the building and district scales.

To illustrate the cumulative building-scale implications of linear thermal transmittance, Figure 10 presents the additional heat transfer per unit temperature difference (ΔQ) shown by EQ (9) as a function of façade glazing perimeter length (L) according to ISO 10211 [19], [20]. Where ΔQ represents heat transfer per unit temperature difference (W/K).

$$\Delta Q = \psi \ L. \ldots \qquad \ldots \text{EQ (9)}$$

The comparison between a conventional aluminum spacer (ψ = 0.061 W/(m·K)) and a representative warm-edge spacer (ψ = 0.030 W/(m·K)) demonstrates that linear thermal bridging scales directly with perimeter length. For a high-rise floor with 400 m of glazing perimeter, the conventional spacer results in approximately 24.4 W/K of additional heat transfer, whereas a warm-edge alternative would reduce this value to 12.0 W/K. When multiplied across multiple floors, the cumulative effect becomes substantial, reinforcing the importance of edge detailing in cooling-dominated urban environments. From a broader urban perspective, the results emphasize that façade configuration decisions at the component scale directly influence cumulative cooling demand in high-density glazed developments. Even moderate increases in linear thermal transmittance can scale substantially when multiplied by perimeter length and building height. Therefore, integrating linear thermal metrics alongside conventional area-based U-values is essential for climate-adaptive façade design in hot-arid cities.

Future work will extend the validated workflow to full curtain-wall mullion/transom sections (including thermal-break aluminum profiles where applicable) and perform parametric studies on spacer properties, cavity/radiation assumptions (emissivity), and glazing gas selection to reduce $\boldsymbol{\psi}$ and improve overall system thermal performance. The comparative framework adopted in this study provides a controlled reference methodology for isolating aluminum-driven edge effects in façade assemblies, offering designers a clearer basis for evaluating spacer selection and edge detailing strategies in curtain-wall systems. While the present study focuses

on a representative section, the results highlight cumulative perimeter effects that can scale significantly in dense urban curtain-wall developments.

Abbreviations

Abbreviation	Definition
2D	Two-Dimensional
bf	Projected frame width
bg	Visible glazing width
bp	Visible panel width
CFD	Computational Fluid Dynamics
COMSOL	COMSOL Multiphysics® Modeling Software
dg	Total glazing thickness
dp	Panel thickness
dt	Glass thickness (single pane thickness)
DGU	Double-Glazed Unit
EPDM	Ethylene Propylene Diene Monomer (gasket material)
ha	Convective/conductive heat-transfer coefficient in cavity
he	External surface heat-transfer coefficient
hi	Internal surface heat-transfer coefficient
hr	Radiative heat-transfer coefficient
k	Thermal conductivity
keq	Equivalent thermal conductivity (cavity)
L	Glazing perimeter length
L_2D	Two-dimensional thermal conductance
PDM	Pollution Degradation Modifier
Rs	Surface thermal resistance
Rsi	Internal surface thermal resistance

Rse	External surface thermal resistance
Ti	Interior air temperature
Te	Exterior air temperature
Ug	Centre-of-glazing thermal transmittance
Up	Centre-of-panel thermal transmittance
Uf	Frame thermal transmittance
ψ	Linear thermal transmittance
Φ	Total heat flow rate per unit depth
ΔQ	Additional linear heat transfer per unit temperature difference
ΔT	Temperature difference

Declarations

- **Conflicts of Interest:** The authors declare no conflicts of interest.
- **Supplementary Materials:** The data and materials used in this study are included within the manuscript.
- **Author Contributions:** Both authors equally contributed to the study.
- **Funding:** This research received no external funding.
- **Institutional Review Board Statement:** Not applicable.
- **Informed Consent Statement:** Not applicable.
- **Ethics declaration:** Not applicable.
- **Data Availability Statement:** The data and materials used in this study are included within the manuscript.
- **Acknowledgments:** NA.

References

[1] M. Malvoni, C. Baglivo, P. M. Congedo, and D. Laforgia, "CFD modeling to evaluate the thermal performances of window frames in accordance with the ISO 10077," *Energy*, vol. 111, 2016, doi: 10.1016/j.energy.2016.06.002.

[2] I. I. Mitin, "EN ISO 10077-1 Thermal performance of windows, doors and shutters - Calculation of thermal transmittance - Part 1: General (ISO 10077-1:2017)," *Tselliuloza, Bumaga, Karton/Pulp, Paper, Board*, no. 5, 2017.

[3] M. T. Naqash, "Analyzing Glass Configurations For Energy Efficiency In Building Envelopes: A Comparative Study," *Journal of Applied Science and Engineering*, vol. 28, no. 2, pp. 319–333, 2025, doi: 10.6180/jase.202502_28(2).0011.

[4] L. Yu, C. Lin, W. Gu, X. Zheng, Y. Zhang, and P. Shen, "Passive design strategies for curtain wall system in subtropical office buildings in China considering multi-sensory comfort," *Energy and Built Environment*, Jan. 2026, doi: 10.1016/J.ENBENV.2026.01.001.

[5] M. A. Mohammed, I. M. Budaiwi, M. A. Al-Osta, and A. A. Abdou, "Thermo-Environmental Performance of Modular Building Envelope Panel Technologies: A Focused Review," 2024. doi: 10.3390/buildings14040917.

[6] X. Li and Y. Wu, "A review of complex window-glazing systems for building energy saving and daylight comfort: Glazing technologies and their building performance prediction," *J. Build. Phys.*, vol. 48, no. 4, 2025, doi: 10.1177/17442591241269182.

[7] J. K. Calautit, H. Sun, J. Li, A. Dik, and M. Mohammadi, "Keeping it simple: Field testing and techno-economic assessment of a low-cost secondary quad glazing for enhanced energy efficiency in buildings," *Energy and Built Environment*, 2025, doi: 10.1016/j.enbenv.2025.03.004.

[8] J. L. Toroxel, S. M. Silva, and J. Fernandes, "Contribution of Glazed Balconies as a Passive Heating System in Contemporary Buildings in Northern Portugal," *Sustainability (Switzerland)* , vol. 16, no. 13, 2024, doi: 10.3390/su16135658.

[9] P. Montero-Gutiérrez, J. S. Ramos, Mc. G. Delgado, D. C. Medina, T. P. Amores, and S. Á. Domínguez, "Thermal comfort and energy performance of a passive urban climate shelter under extreme heat: Large-scale measurements at Cartuja Qanat Agora," *Build. Environ.*, vol. 296, p. 114550, May 2026, doi: 10.1016/J.BUILDENV.2026.114550.

[10] N. Das, R. Elangovan, P. S. Chani, S. Kumar, and P. Vaidya, "The transforming thermal performance of residential buildings in the lower Himalayan cold climatic region," *Build. Environ.*, vol. 286, p. 113686, Dec. 2025, doi: 10.1016/J.BUILDENV.2025.113686.

[11] J. Kim, B. Meller, J. Woo, A. S. Arora, and T. Schuetze, "Integrated Urban Climate Resilience and Sustainability Assessment System for Urban Regeneration and Building Renovation," *Land (Basel).*, vol. 15, no. 6, p. 920, May 2026, doi: 10.3390/land15060920.

[12] Z. Xu, T. Georgiadis, L. Cremonini, S. Marini, F. Ravaldi, and S. Toselli, "Microclimate Impacts of Urban Green Redevelopment: A Thermal Comfort Simulation in Imola, Italy," *Land (Basel).*, vol. 15, no. 6, p. 942, May 2026, doi: 10.3390/land15060942.

[13] Y. Fang, Z. Liu, Y. Jia, M. Ke, R. Yang, and Y. Cai, "Impact of Urban Block Morphology on Solar Availability in Severe Cold High-Density Cities: A Case Study of Residential Blocks in Harbin," *Land (Basel).*, vol. 14, no. 3, Mar. 2025, doi: 10.3390/land14030581.

[14] A. Formisano and M. T. Naqash, "Glass panels supported by spider fittings: advantages, challenges, and applications in modern masonry façades," *International Journal of Masonry Research and Innovation*, vol. 1, no. 1, 2024, doi: 10.1504/ijmri.2024.10063211.

[15] M. T. Naqash and A. Formisano, "Assessment of cantilevered curtain wall system supported by tension rods for an enclosed circular building," *Structures*, vol. 68, no. May, p. 107133, 2024, doi: 10.1016/j.istruc.2024.107133.

[16] A. Formisano and M. T. Naqash, "Innovative reinforced aluminium alloy curtain walls: Numerical analysis and experimental validation," *Journal of Building Engineering*, vol. 117, 2026, doi: 10.1016/j.jobe.2025.114554.

[17] M. T. Naqash and A. Formisano, "A Conceptual Framework for Pollution-Resilient Aluminium Façades: Introducing the Pollution Degradation Modifier (PDM)," *Buildings*, vol. 16, no. 4, Feb. 2026, doi: 10.3390/buildings16040861.

[18] COMSOL, "COMSOL Multiphysics® Modeling Software," Comsol.

[19] EN ISO 10211, "Thermal bridges in building construction — Heat flows and surface temperatures — Detailed calculations," 2017.

[20] T. G. Theodosiou and A. M. Papadopoulos, "The impact of thermal bridges on the energy demand of buildings with double brick wall constructions," *Energy Build.*, vol. 40, no. 11, 2008, doi: 10.1016/j.enbuild.2008.06.006.